In vitro and *in vivo* evaluation on the bioactivity of ZnO containing nano-hydroxyapatite/chitosan cement

Zhang Li,[1] **Li Yubao,**[1] **Zuo Yi,**[1] **Wu Lan,**[1] **John A. Jansen**[2]

[1]*Analytical and Testing Center, Research Center for Nano-biomaterials, Sichuan University, Chengdu 610064, People's Republic of China*

[2]*Department of Periodontology and Biomaterials, Radboud University Nijmegen Medical Center, P.O. Box 9101, 6500 HB Nijmegen, The Netherlands*

Abstract: A ZnO containing nano-hydroxyapatite/chitosan (n-HA/CS) cement was developed and its bone formation ability was investigated *in vitro* and *in vivo*. The physico-chemical properties of the cement were determined in terms of pH variation during and after setting, injectability and wettability. The results indicated that, the pH varied from 7.04 to 7.12 throughout the soaking of the cement in distilled water. The injectability was excellent during the first 4 min, but the cement became less injectable or even not injectable at all after 7 min setting. The static contact angle of the cement against water was $53.5 \pm 2.7°$. The results of immersion tests in simulated body fluid (SBF) indicated that the cement exhibited excellent bone-like apatite forming ability. *In vivo* studies, involving the installation of the cement of tibial-bone defects in rabbit tibia revealed an inflammatory response around the cement at 3 days of implantation. After 4 weeks, the inflammation began to disappear and the cement had bound to the surrounding host bone. Radiological examination also confirmed that the ZnO containing n-HA/CS cement significantly induced new bone formation. These results suggest that the ZnO containing n-HA/CS cement may be beneficial to enhance bone regeneration in osseous defect sites. © 2009 Wiley Periodicals, Inc. J Biomed Mater Res 93A: 269–279, 2010

Key words: ZnO; nano-hydroxyapatite; chitosan; cement; bone formation

INTRODUCTION

Hydroxyapatite (HA) with chemical and crystallographic similarity to the apatite in human bone and teeth can form a direct chemical bond with surrounding bone tissue and therefore has been used extensively in orthopedics and bone regeneration.[1–3] However, a major disadvantage of sintered HA blocks is that it exists in a bulk form, requiring surgeons to fit the surgical site around the implant or to carve the graft to the desired shape,[4] while HA in the form of particles has a tendency to migrate from the implantation site.[5] Due to these reasons, the therapeutic effects of HA tend to be deteriorated in clinic. Therefore, developing a new kind of material with moldability and *in situ* self-hardening ability and, at the same time maintenance of the material in the defect site is desirable and necessary for orthopedic repair.

Currently, natural polymers have been paid a great deal of attention by many researchers owing to some of their unique properties, such as nontoxicity, degradability, and good biological compatibility.[6–9] Chitosan (CS) is an N-deacetylated form of chitin and has various degrees of substitution for N-acetyl groups. It has been proven that CS can degrade *in vivo* into nonharmful and nontoxic products[10–12] and thus has been used in many biomedical applications, including wound dressings and drug or gene delivery.[13] In addition, a large amount of amino groups present in the chains give CS high positive charges, through which CS can bind tightly with negatively charged cells via electrostatic interaction.[14,15] When applied to bone defects in animal models, CS was found to improve osteogenesis and angiogenic activity.[16,17] However, the poorer mechanical strength of CS makes it impossible to bear the load that bone is usually subjected to and thus, it tends to collapse.

Accordingly, inorganic–organic composites for bone repair should be developed and are expected to enhance the mechanical properties of the polymer matrix with particle reinforcement and to reduce the

---

Correspondence to: L. Yubao; e-mail: nic7504@scu.edu.cn

disadvantages associated with the individual component as well as to improve the overall biological response to the implant.[18–21] Nano-hydroxyapatite/ Chitosan (n-HA/CS) composites have been studied extensively and proved to combine the advantages of the two included components.[19,22–24] However in a previous study, the incorporation of zinc oxide (ZnO) has been proven to shorten the setting time and enhance the mechanical strength and to improve the bioactivity and antibacterial activity of n-HA/CS composite.[25]

As a consequence, in the current study the *in vitro* bioactivity and *in vivo* biological response of ZnO containing n-HA/CS composite was investigated further.

MATERIALS AND METHODS

Chitosan was obtained from Haidebei Co. (Jinan, China). The degree of deacetylation was 80% and the weight-averaged molecular weight was about 250,000. All other chemicals are of analytic grade and used as received. The n-HA/CS composite powder was synthesized by the coprecipitation method described detailed in the Ref. 27.

Composition of n-HA/CS composite cement

The fast-setting cement was mainly composed of a powder phase containing n-HA/CS (70 wt % n-HA) composite and a liquid phase comprised of 2 wt % citrate acid, 1 wt % NaH_2PO_4, and 1 wt % $CaCl_2$ aqueous solution. The powder phase also contained 8 wt % ZnO used as a setting accelerator and the precise concentrations of n-HA, CS, and ZnO in the final powder mixture were 64.4, 27.6, and 8 wt %, respectively. According to the previous research,[25] the liquid/powder (L/P) ratio of 1.0 mL/g was selected to be used in this study. The cement paste was prepared by mixing the powder with liquid for 20 sec by hand. The paste was then used to prepare samples for evaluating their properties.

pH variation during and after setting

Two grams of cement powder was mixed with 2 mL liquid at room temperature for about 20 sec and the paste was quickly transferred into a plastic mold with a closed bottom. The mold was then immersed for 60 h in 50 mL of distilled water at 37°C under gentle stirring at 200 rpm. The pH of the distilled water was measured which a compact type pH meter at 5-h intervals. The obtained pH data were the average values of three measurements.

Injectability

Injectability is described as the weight loss percentage (I%) between the cement paste extruded from the syringe to the cement paste remaining inside the syringe. To measure the injectability of the cement, a method was used as proposed by other authors.[26,40] Three grams of cement were transferred to a 5-mL disposable syringe with a nozzle diameter of 2.0 mm and then extruded through the nozzle at a crosshead speed of 15 mm/min, using a peak load of 100 N in a Universal Testing Machine. Measurements were repeated three times for reproducibility. Finally, the injectability was determined as follows:

$$1\% = 1 - ((\text{the mass of cement remaining in the syringe/} \\ \text{the starting cement mass}) \times 100\%) \quad (1)$$

Wettability

The static contact angle of n-HA/CS cement was measured using a contact angle goniometer (Model JY-82; Chengde Experimental Machine Plant, China). Distilled water was dropped onto the surface of the cement pellet before measuring. The data presented were the mean value of at least six independent measurements.

In vitro behavior

Simulated body fluid (SBF) was used for *in vitro* bioactivity experiments. SBF, proposed by Kokubo and coworkers,[27] was prepared by dissolving reagent-grade chemicals of NaCl, $NaHCO_3$, KCl, $K_2HPO_4·3H_2O$, $MgCl_2·6H_2O$, $CaCl_2·2H_2O$, Na_2SO_4, and tris(hydroxymethyl)-aminomethane into distilled and deionized water and buffered to pH 7.4 at 37°C with hydrochloric acid and has ion concentrations that are nearly the same as those of human blood plasma.

Cement specimens with dimensions of Φ 10 × 1 mm were immersed in plastic tubes containing 15 mL of SBF. The tubes were sealed to minimize the change in pH and incubated in a water bath at 37°C under gentle reciprocal motion. The samples were incubated in SBF for 1, 2, 4, 6, and 8 weeks, respectively, and the SBF was changed every 7 days. After the different periods of immersion time, specimens were removed out from SBF, rinsed with distilled water and dried prior to analysis.

The samples were gold coated under an argon atmosphere using a sputter coater and were examined using a JEOL JSM5600LV scanning electron microscope (SEM). The aggregations deposited on the surface of the samples were analyzed by an energy dispersive X-ray analyzer (EDX, PV9100-65), which was directly connected to the SEM. The concentrations of Ca and P ions in SBF after immersion were determined by an inductively coupled plasma atomic emission spectrometer (ICPS-7500). All reported data were the average value of five tests.

In vivo evaluation

To investigate the *in vivo* bone forming ability of the ZnO containing n-HA/CS cement, preharedened cement samples were implanted into the tibial bone of rabbits. In
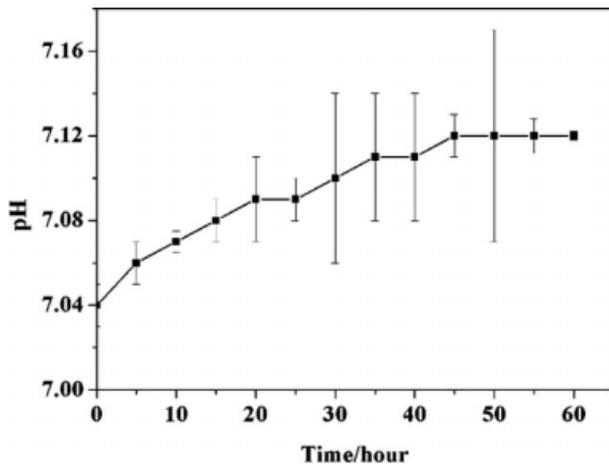
Figure 1. pH variation with the soaking time of the cement in distilled water.

this study, 24 New Zealand white rabbits (2.0–3.0 kg) were assigned randomly to one of four groups designating as 3-day, 4-, 8-, and 12-week groups. Each group consisted of six rabbits. The hind limbs of the rabbits were shaved and disinfected after induction of general anesthesia with a mixture of 10% ketamin hydrochloride and xylazinehydrochloride (3 mL/kg). Subsequently, a vertical incision was made to disclose the skin and periosteum and the tibia was exposed. A hole with a diameter of 5 mm and depth of 8 mm was drilled in the proximal epiphysis of the tibia. After rinsing in order to remove bone fragments, in 20 rabbits the tibial defects were filled with prehardened samples, while the defects in the other four rabbits were left empty and used as controls. Finally, the wounds were sutured with silk threads and then disinfected. After the animals were recovered from anesthesia, they were allowed free movement in their cages.

The rabbits were sacrificed at 3 days, 4, 8, and 12 weeks post operation. X-ray radiographs of the rabbit tibias with the implanted materials were taken using a Philips 1025 X-ray Radiograph System (Japan). The femurs with implants were dissected free of soft tissues and fixed with 10% neutral buffered formalin for 24 h. Fixed specimens were decalcified in general acidic decalcifying solution for 72 h, embedded in paraffin wax, cut into 7-μm sections and stained with Masson trichrome (M-T) as well as hematoxylin and eosin (HE) for light microscopic examination.

RESULTS

pH variation during and after setting

Figure 1 shows the pH variation of the distilled water during soaking of the cement paste. The measured pH was 7.04 just after immersion and subsequently increased gradually to 7.12 after 45 h. Thereafter, the pH of the distilled water remained almost constant.

Injectability assay

The variation of injectability against time is plotted in Figure 2. It is obvious that the injectability of the cement was higher during the first 4 min of setting and, after this time, the cement shows to be less injectable. Injectability decreased drastically after 7-min setting due to the high viscosity of the paste and at 9 min, the cement was practically no longer injectable.

Wettability

The static contact angle reflects directly the wettability of a material. In general, the smaller the contact angle of a material against water, the better the wettability of the material is, that is to say, the material is more hydrophilic. In this experiment, the static contact angle of the cement against water is 53.5 ± 2.7°, which is relatively small, meaning that the cement has good hydrophilicity.

In vitro behavior

Figure 3 shows the SEM photos of the cement after being immersed in SBF for different periods of time, in which the over-right insets are the photos with high magnification. It can be seen from Figure 3 that the nucleation of Ca–P granulates has taken place during the first week of immersion and many Ca–P spherical particles deposited on the cement surface, as has been reported elsewhere.[58–62] After 2 weeks, the number and size of the Ca–P particles deposited on the cement surface increased and there were large number of islands of Ca–P whose diameters enlarged continuously, as shown in Figure 3(b–d).
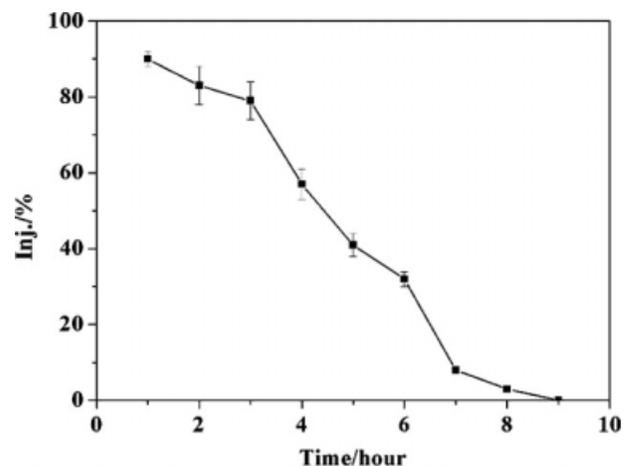

Figure 2. The variations of injectability of the cement against the setting time.
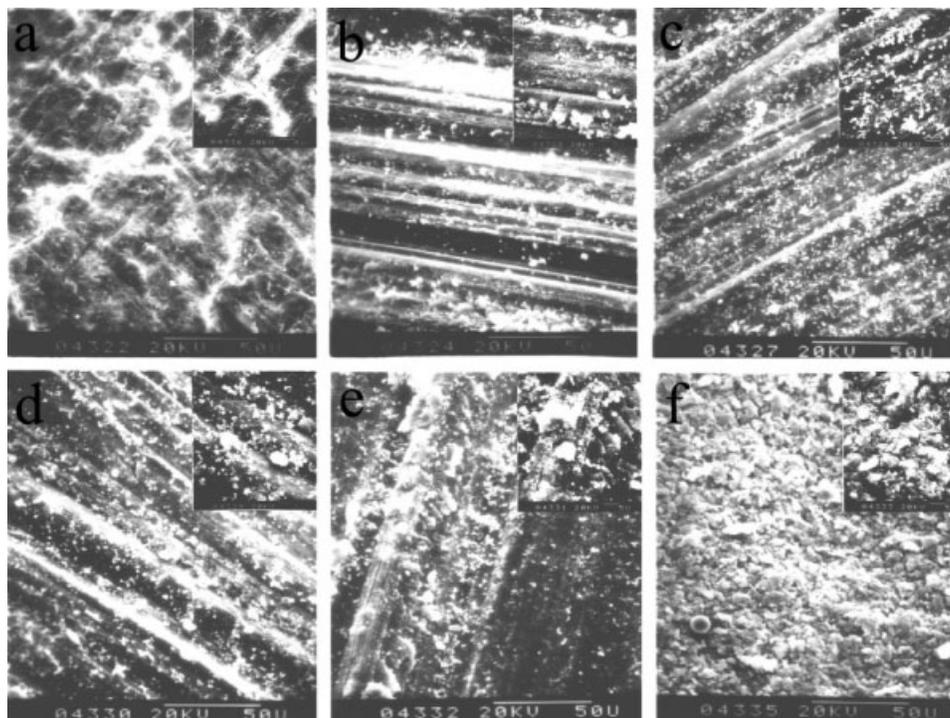
Figure 3. SEM photos of the cement immersed in SBF for different periods of time: (a) before immersion; (b) 1 week; (c) 2 weeks; (d) 4 weeks; (e) 6 weeks, and (f) 8 weeks.

At 8 weeks of immersion, the growth and coalescence of Ca–P particles continued and then formed a Ca–P layer covering on the specimen surface, as displayed in Figure 3(e). These Ca–P particles or layers are apatite according to EDX analysis, same as those reported elsewhere.[58–62]

The concentrations of Ca ion and P groups in SBF as a function of the immersion time were plotted in Figure 4. It was demonstrated that the concentration of Ca ion dropped from 83.23 to 74.89 ppm dramatically during the first week of immersion, then rebounded till 2 weeks. After that, the concentration of Ca ion descended continually, as shown in Figure 4(a). It could be found from Figure 4(b) that the concentration of P groups in SBF declined all through the immersion. But it is noticeable that the concentration of P groups decreased rapidly at the first week and since then, decreased steadily. According to the above mentioned, it could be concluded that, the initially fast decreases in the Ca and P ion concentrations might have been due to the adsorption of these ions to the chitosan surface and the rapid deposition of Ca and P ions on the cement. Then, the fact that Ca concentration rebounded till the second week might be induced by the continuous dissolution of the n-HA in the cement as well as the contribution of the small amount of P groups from cement liquid. After that, the gradual decrease of the Ca concentration suggested that the microenviron-ment with high Ca and P concentrations around the cement accelerated the agglomeration of Ca–P deposit, and thus dropped the Ca concentration in the solution continuously. In comparison, the P concentration remained the descending trend throughout the immersion. However, the changing trend of the P concentration indicating the quick accumulation of Ca–P deposits at the first week, and also proved that the deposition process proceeded all through the immersion period.
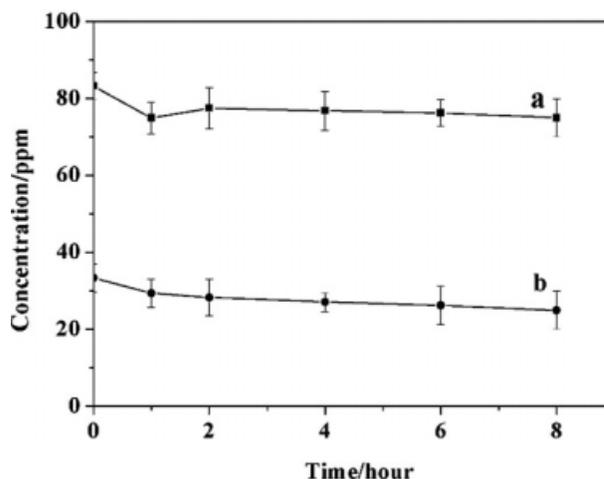

Figure 4. The content of Ca (a) and P (b) in SBF solution as a function of the immersing time.
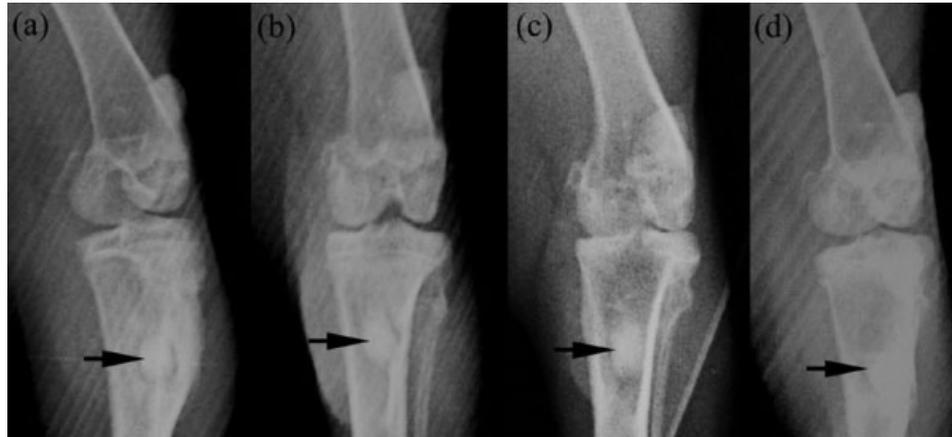
Figure 5. Radiographs of the cement after implantation: (a) 3 days; (b) 4 weeks; (c) 8 weeks, and (d) 12 weeks.

In vivo evaluation

Macroscopic inspection and radiological examination

It was found that these rabbits began to move about 3 days postoperatively and appeared no post-operative complications. The implants connected with the surrounding bone tissues tightly at 4 weeks implantation and were hard to be taken out. After 8 weeks, the implants combined with the around tissues more tightly and these wounds healed gradually. Although 12 weeks after implantation, a large amount of new bone formed surrounding these implants and the tubercle at the tibia grew thicker, in which these implants were encapsulated entirely.

The sequential radiological changes in the healing areas are shown in Figure 5. On the third day, bone density around the implant decreased markedly, behaving a distinct radiolucent area, which indicated a larger gap between the implant and the around tissues [Fig. 5(a)]. After 4 weeks, there was still a radiolucent region around the implant, but it became blurred, implying that the margin of the cement began to be adsorbed and replaced by a little amount of newly formed bone [Fig. 5(b)]. The radiolucent area became gradually indistinct and a discrete bone neoformation became more clearly defined with a bone wall and a clear osteosclerotic reaction, suggesting that adsorption of the cement was still continued and, the cement integrated with the surrounding bone gradually, as shown in Figure 5(c). Bone formation continued and at week 12, the implant density was very similar to the surrounding bone, implying that the newly formed bone filled completely the interfacial crevices between the cement and the host bone as well as the adsorbed sites for the cement.

Histological observation

At 3 days after implantation, a local accumulation of polymorphonuclear leucocytes and bone trabeculae fractures with hemorrhagic areas were observed as normal consequences of surgical trauma, as shown in Figure 6. In contrast, the control defect was filled with a coagulum (not shown here).

At 4 weeks of implantation, light microscopic image of decalcified section with HE staining showed that a thin layer of connective tissue surrounded the implant and newly formed woven bone loosely arranged at the outer of the layer, meanwhile, chitosan degradation took place and some crevices appeared on the surface of the implant, and these sites were infiltrated with fibrous tissue [Fig. 7(a)]. M-T staining also indicated that loosely collagenous tissue, which was stained blue, was deposited surrounding the implant, suggesting the formation of new bone, as shown in Figure 7(b). In the control defect without cement implantation at 4 weeks [Fig. 7(c)], connective tissue spanned the host bone margin and the defect was completely filled with fibrous connective tissue. However, negligible amount of new bone was observed.

After 8 weeks of surgery, the connective tissue layer almost disappeared and extensive new bone formation was seen in the gap between the host parietal bone and the cement, implying that bone integration was the main biological activity in this period [Fig. 8(a)]. Apart from this, bone growth took place centripetally toward the degraded sites and the crevices in the implant. Part of the newly formed woven bone showed lamellar-like structures and became more mature, which could be clearly observed in Figure 8(b). At this period, although new bone was rapidly formed, complete reunion of new bone had not occurred. In the control, the scar
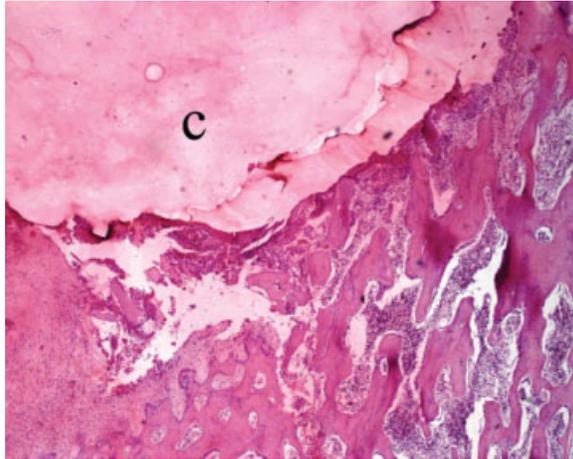
Figure 6. Light micrographs of tissue responses around the cement implant for 3 days. HE staining (×200); C, cement. [Color figure can be viewed in the online issue, which is available at www.interscience.wiley.com.]

tissue was mainly fibroblasts that had multiplied upon the defect with newly formed capillaries, as shown in Figure 8(c).

At 12 weeks after implantation, new bone progressively formed around the implant. Mineral trabeculae dispersed randomly around the implant, began to link together and at the same time, densely mature lamellar bone could also be observed. In

addition, a lot of blood vessels were found to infiltrate into the newly formed trabeculae [Fig. 9(a)]. Collagen deposition increased significantly at 12-week postoperation and in Figure 9(b), chitosan was stained dark red, whereas collagen deposition appeared as dense blue staining, demonstrating that new bone remodeling had occurred at this stage. In comparison, microscopic examination on the control after 12 weeks of implantation [Fig. 9(c)] showed that the defect was still filled with fibrous scar tissue, which was similar to that observed in the control at 8-week post operation, no newly-formed bone could be seen at the center of the defect.

DISCUSSION

A cement for use in clinical practice must have good handling, appropriate setting time, as well as suitable pH and wettability.[28] It has been reported that pH during the hardening process will influence tissue reaction to the cement.[29] Acidic conditions tend to induce aseptic inflammatory response of surrounding tissue.[30] In addition, pH may also influence the surface chemistry, thereby affects the biological response, such as proliferation and spreading of cells.[31] Chou et al.[32] have described the effect of different initial pH of SBF causing morphological

Figure 7. Light micrographs of tissue responses around the cement implants and the control for 4 weeks: (a) HE staining (×200); (b) Masson staining (×200), and (c) HE staining of the control (×200). C, cement. [Color figure can be viewed in the online issue, which is available at www.interscience.wiley.com.]
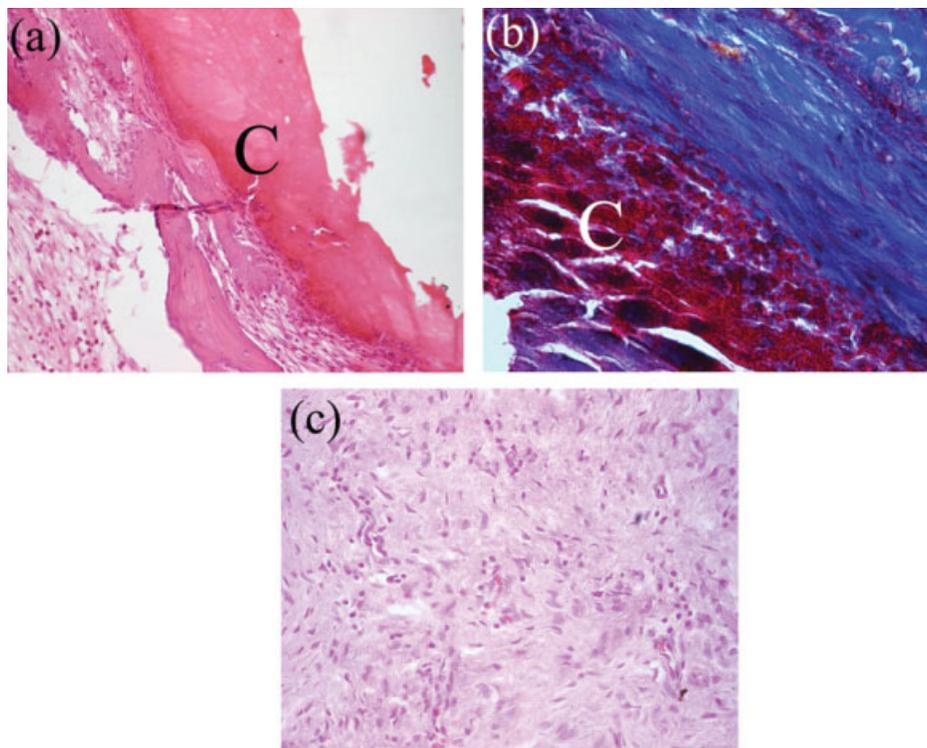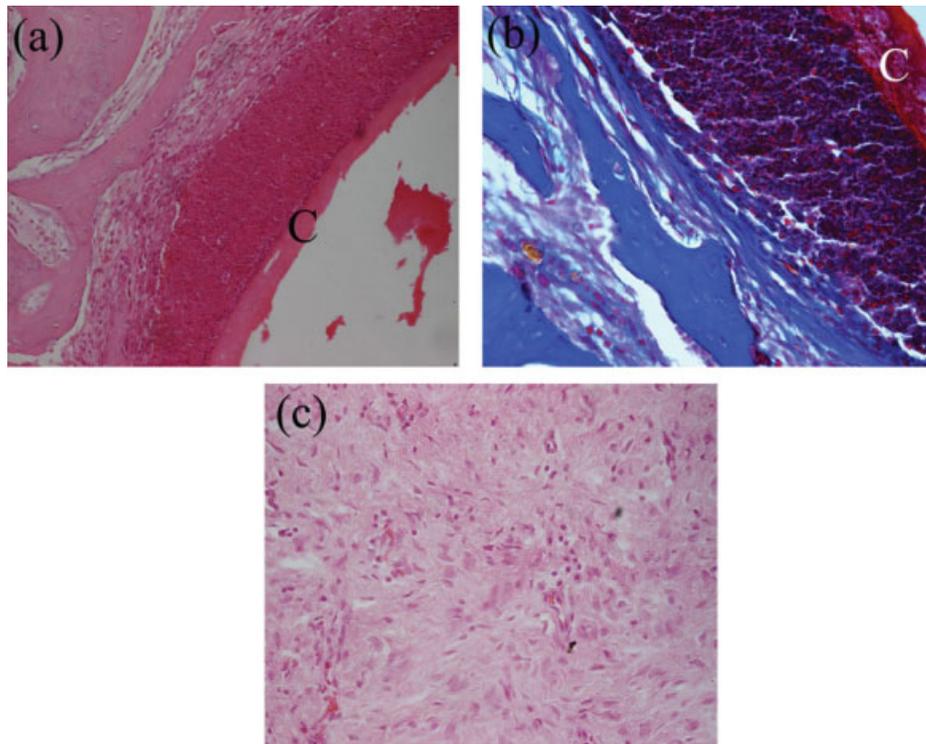
Figure 8. Light micrographs of tissue responses around the cement implants and the control for 8 weeks: (a) HE staining (×200); (b) Masson staining (×200), and (c) HE staining of the control (×200). C, cement. [Color figure can be viewed in the online issue, which is available at www.interscience.wiley.com.]

Figure 9. Light micrographs of tissue responses around the cement implants and the control for 12 weeks: (a) HE staining (×200); (b) Masson staining (×200), and (c) HE staining of the control (×200). C, cement. [Color figure can be viewed in the online issue, which is available at www.interscience.wiley.com.]
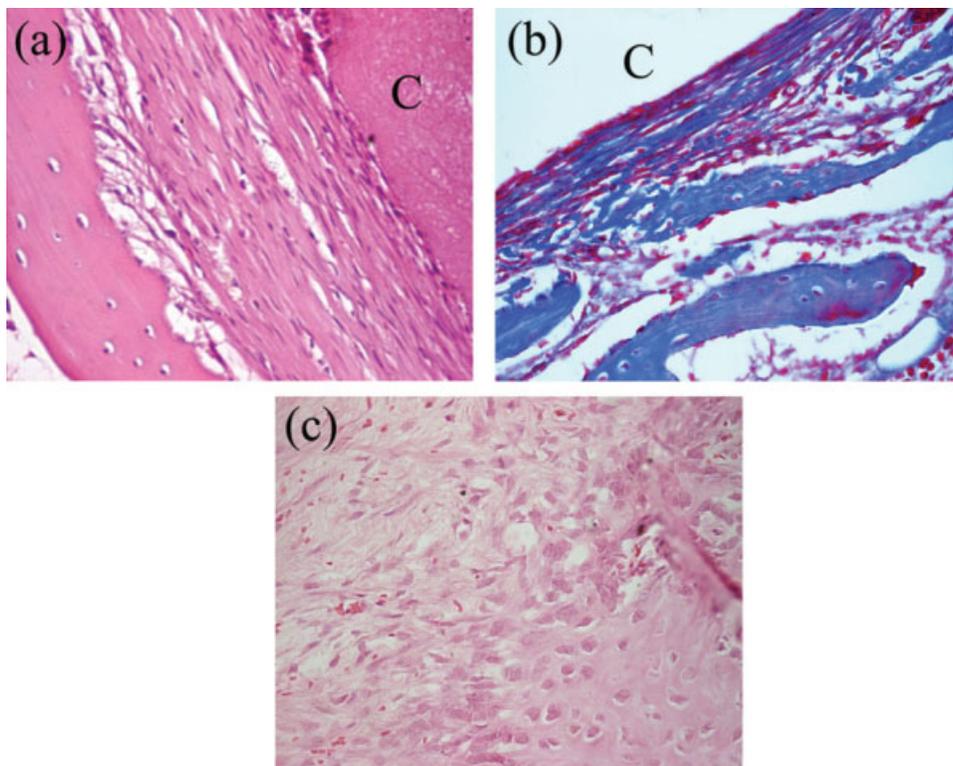
difference in the accelerated biomimetic apatite, and reported that higher initial pH promotes faster precipitation of precursor spheres which are comprised of fewer stable, and more unstable phases which will subsequently undergo rapid phase transformation into large platelike structures, while micro- and nano-topography has also been shown to alter cellular morphology, cytoskeleton and proliferation. In this study, pH value of the cement during and after setting varies from 7.04 to 7.12 during the immersion of $0 \sim 45$ h, after that the pH remains about 7.12, which is very close to the pH of human body fluid (about 7.25). The slightly basic environment would be expected to alleviate the inflammatory response, and also accelerate the deposition of bone-like apatite[33] and the differentiation, spreading, and proliferation of osteoblasts, and thus facilitate defect repair.

The applicability of injectable self-setting biomaterials is largely dependent on its self-setting characteristics, such as injectability and setting times. Often, injectability properties of cements are characterized by extrusion tests. According to the results reported by other authors[34,35] the more cement could be extruded, the more injectable the cement was. Generally, cements intended for filling irregular bone defects must be fluid, also they should have enough consistency to prevent early leakage of the cement. Furthermore, the time of injection should last enough to permit the injection without additional problems. However, many reports have shown that improving the injectability of the cement paste can inadvertently prolong the cement setting time.[36–38] For example, the use of trisodium citrate solution instead of water improved the injectability of a CPC greatly, but significantly increased its setting time.[26] A long setting time could cause problems because of the cement's inability to support stresses within this time period. For instance, a severe inflammatory response occurred when the CPC failed to set and disintegrated, likely due to a low initial mechanical strength.[36,38] In the present study, it can be seen from Figure 2 that there has a sharp decrease for the injectability after setting for 7 min, meaning that before 7 min the cement is relatively workable, after that it is hard to handle. The injection time is regarded as a consequence of the viscosity increase and viscoelastic behavior of the cement during setting.[39,40] Some authors have defined a "dough-time D" as the time when injectability decreases drastically as a function of the injection time.[41] Hereby, it can be concluded that the setting time of 7 min should be referred as *the dough-time D* for the so obtained cement in the paper.

Wettability is perhaps one of the most important factors determining the quantity and quality of adsorbed proteins and the biocompatibility, and that the static contact angle reflects directly the wettability of a material.[42,43] The static contact angle has been proven to be the most significant determinant of adhesion strength and, in turn, the cell growth rate depends on the adhesion strength.[44] Osteoblasts preferentially adhere onto surfaces of biomaterials with the similar wettability to themselves. The average contact angle of a water droplet on an osteoblast monolayer was reported to be $26.9 \pm 0.3°$, and the contact angles of bone biomaterial like sandblasted titanium and hydroxyapatite to be 41 or 43°, respectively.[43] Whereas, the contact angle of the cement against water in this study is $53.5 \pm 2.7°$. So, it can be postulated that osteoblasts will preferentially adhere onto the surface with similar wettability. Therefore, the cement is favorable to the protein adsorption and osteoblast adhesion, while cell adhesion is regarded as a crucial phase in many biological processes and primarily in tissue repair.

Generally, artificial materials implanted into bone defects are encapsulated by fibrous tissue isolated from the surrounding bones. It has been reported, however, during the recent years that some bioactive ceramics, for example, Bioglass, sintered hydroxyapatite, and glass-ceramic A-W, bond to living bone without forming fibrous tissue around them, which when implanted into bone defects, forms spontaneously a layer of biologically active bonelike apatite on their surfaces to induce chemical integration of bone tissue.[1,2,45,46] It is a common notion that bone-like HA plays an essential role in the formation, growth, and maintenance of the bone tissue–biomaterial interface, and this bone-like apatite layer can be reproduced *in vitro* at physiological temperatures in simulated body fluid (SBF),[47–49] a solution with ion concentrations and a pH value similar to those of human blood plasma. In this study, the SEM observation (Fig. 3) indicated that apatite started to precipitate after 1 week of immersion in SBF and the spherulites increased in both number and size with immersion time, which is similar to that reported by others,[50] suggesting the cement exhibits high bioactivity. In addition, the results of the Ca and P concentration variations (Fig. 4) provided further evidence that bone-like apatite formed on the cement in the first week of soaking. In the recent years, microcrystalline HA powders have been employed as seeds for the apatite evolution in CPCs due to HA seeds providing sites for heterogeneous nucleation.[51] Yang et al.[52] have also reported that addition of apatite seeds into the starting CPC powder mixture does promote the formation of deposited apatite as they themselves provide nucleation sites for HAp crystal growth. For this reason, it can be inferred that the n-HA granules in the present cement powder may serve as nucleation sites for apatite precipitation. During the immersion, the dissolution of n-HA and the contribution of additional small

amount of PO_4^{3-} and Ca^{2+} lead to the precipitation of apatite, once the main ionic species, such as Ca^{2+} and PO_4^{3-}, supersaturate the solution. Furthermore, data in the literature show that the rate of apatite formation can be increased by the presence of phosphate in the solution.[53,54] Also, it has been reported that the high surface charge density of chitosan can attract the adsorption of Ca and P ions on its surface.[55,56] Although Wan et al.[57] have reported that the hydroxyl groups of the acetyl glucosamine residues on chitin are able to bind both Ca and P ions in a loose fashion, increasing the degree of supersaturation in the vicinity of the substrate. When the local degree of supersaturation is high enough, the critical radius for nucleation is achieved and Ca–P nuclei are formed. Once the apatite nuclei are formed, they can spontaneously grow by consuming the Ca and P ions in the SBF, as the SBF is already supersaturated with respect to the apatite even under normal conditions.[58] Further growth of crystals takes place when supernatant ions fill the lattice sites predetermined by the initially formed nuclei. This outward growth from a point leads to the observed spherical morphology of the deposits, which was also reported elsewhere. Similar nucleation of Ca–P deposits was also observed for the ZnO containing n-HA/CS cement incubated in SBF in this study. We could observe that the deposition of Ca and P ions occurred during the first week of immersion, and the spherical Ca–P deposits increased and agglomerated with soaking time. With the immersion time and the incorporation of other ions, these Ca–P deposits underwent a series of compositional adjustments and phase structural variations, and ultimately changed into bone-like apatite layer. In addition, the high apatite-forming ability of the present cement might be relevant to the incorporation of ZnO in the cement powder. It is well known that zinc (Zn), titanium (Ti), tantalum (Ta), and zirconium (Zr) are all belonging to the family of transitional metals, and extensive studies have indicated that Ti, Ta, and Zr enable the formation of bone-like apatite on their surfaces in SBF through the catalytic effect of the Ti—OH,[59] Ta—OH[60,61] and Zr—OH[62] groups, respectively. Therefore, it can be postulated that, when ZnO encounters with aqueous solution, plenty of Zn—OH groups will be formed and act as the apatite nuclei, and thus trigger the formation of bone-like apatite on the surface of n-HA/CS cement in SBF.

Our original motive of introducing ZnO into the cement was to shorten the setting time and reinforce the cement, and the obtained results were also desirable, which has been reported previously.[25] However, the effects of ZnO on the biological role of the cement in the present study have also become an important topic in the research field of bone formation recently. Zn is an essential trace element having stimulatory effects on bone formation *in vitro* and *in vivo*.[63,64] Zn^{2+} was also found to increase bone protein, calcium content, and alkaline phosphatase activity in rat calvaria *in vitro*.[65] Ito et al.[66–69] prepared Zn containing apatite ceramics and found that Zn^{2+} release enhanced osteoblastic cell proliferation and differentiation *in vitro* and also promoted bone formation *in vivo*. In the study, ZnO in the cement powder can react with water or acid and release a lot of Zn^{2+}, which may help facilitate more rapid new bone formation and thus accelerate bone defect repair. It could be seen from Figure 5 that bone neoformation around the implant was prominent, and at 12 weeks after surgery the gap between the implant and host bone was almost completely filled with new bone. The process of bone neoformation is more evident if observed from the light micrographs, as shown in Figures 6–9. These results are similar to those reported by Ooms[70] for implants in the cortical bone in goats and Wang[71] for implants in the radii and tibia of rabbits. However, inflammatory and foreign body responses were observed around the cement at 3 days of implantation. Miyamoto et al. reported severe inflammation around calcium phosphate cement implanted immediately after mixing.[72] They proposed that the severe inflammatory was the result of a decrease of transformation to HA and the crumbling of the cement. In this study, the inflammatory may be caused by the crumbling of the cement or/and the excessive ZnO introduced into the cement powder. But it is obvious that the inflammation response was alleviated to a great extent with the implantation time, and till 4 weeks was almost not observed. In the study, although we found the degradation and new bone replacing of the ZnO containing n-HA/CS cements, the duration of the experiment was relatively too short to investigate the resorption of the cement in details. Thus, further experiments are necessary to investigate it.

CONCLUSIONS

In conclusion, our newly developed ZnO containing n-HA/CS cement showed excellent osteoconductivity over a 12 weeks implantation period. However, it will be necessary to carry out further experimental research to validate the clinical use this material in future.

References

1. Brånemark PI. Osseointegration and its experimental background. J Prosthet Dent 1983;50:399–410.

2. Hench LL. Bioceramics: From concept to clinic. J Am Ceram Soc 1991;74:1487–1510.

3. Suchanek W, Yoshimura M. Processing and properties of hydroxyapatite-based biomaterials for use as hard tissue replacement implants. J Biomed Mater Res 1998;13:94–117.

4. Kent JN, Zide MF, Kay JF, Jarcho M. Hydroxyapatite blocks and particles as bone graft substitutes in orthognathic and reconstructive surgery. J Oral Maxillofac Surg 1986;44: 597–605.

5. Wittkampf ARM. Augmentation of the maxillary alveolar ridge with hydroxyapatite and fibrin glue. J Oral Maxillofac Surg 1988;46:1019–1021.

6. Gobin AS, Froude VE, Mathur AB. Structural and mechanical characteristics of silk fibroin and chitosan blend scaffolds for tissue regeneration. J Biomed Mater Res 2005;74A:465–473.

7. Chellat F, Tbrizian M, Dumitriu S, Chornet E, Magny P, et al. In vitro and in vivo biocompatibility of chitosan-xanthan polyionic complex. J Biomed Mater Res. 2000;51:107–116.

8. Denuziere A, Ferrier D, Damour O, Domard A. Chitosan-chondroitin sulfate and chitosan-hyaluronate polyelectrolyte complexes: biological properties. Biomaterials 1998;19: 1275–1285.

9. Wang L, Khor E, Wee A, Lim LY. Chitosan-alginate PEC membrane as a wound dressing: assessment of incisional wound healing. J Biomed Mater Res (Appl Biomater) 2002;63: 610–618.

10. Klokkevold PR, Lew DS, Ellis DG, Bertoami CN. Effect of chitosan on lingual hemostasis in rabbits with platelet dysfunction induced by epoprostenol. J Oral Maxillofac Surg 1992;50:41–45.

11. Khor E, Lim LY. Implantable applications of chitin and chitosan. Biomaterials 2003;24:1339–2349.

12. Kato Y, Onishi H, Machida Y. Application of chitin and chitosan derivatives in the pharmaceutical field. Curr Pharm Biotechnol 2003;4:303–309.

13. Kumar MNVR. A review of chitin and chitosan application. React Funct Polym 2000;46:1–27.

14. Zileinske BA, Aebischer P. Chitosan as a matrix for mammalian cell encapsulation. Biomaterials 1994;15:1049–1056.

15. Zhang M, Li XH, Gong YD, Zhao NM, Zhang XF. Properties and biocompatibility of chitosan films modified by blending with PEG. Biomaterials 2002;23:2641–2648.

16. Muzzarelli RAA, Mattiolibelmonte M, Tietz C, Biagini R, Ferioli G, et al. Stimulatory effect on bone-formation exerted by a modified chitosan. Biomaterials 1994;15:1075–1081.

17. Lee JY, Nam SH, Im SY, Park YJ, Lee YM, Seol YJ, Chung CP, Lee SJ. Enhanced bone formation by controlled growth factor delivery from chitosan-based biomaterials. J Control Rel 2002;78:187–197.

18. Zhang Y, Zhang MQ. Three-dimensional macroporous calcium phosphate bioceramics with nested chitosan sponges for load-bearing bone implants. J Biomed Mater Res 2002;61: 1–8.

19. Hu QL, Li BQ, Wang M, Shen JC. Preparation and characterization of biodegradable chitosan/hydroxyapatite nanocomposite rods via in situ hybridization: a potential material as internal fixation of bone fracture. Biomaterials 2004;25:779–785.

20. Wang JW, Hon MH. Sugar-mediated chitosan/poly(methylene glycol)-β-dicalcium pyrophosphate composite: mechanical and microstructural properties. J Biomed Mater Res 2003; 64A:262–272.

21. Juan P, Isabel IB, Alvaro M, María VR. New method to obtain chitosan/apatite materials at room temperature. Solid State Sci 2006;8:513–519.

22. Wang XH, Ma JB, Wang YN, He BL. Bone repair in radii and tibias of rabbits with phosphorylated chitosan reinforced calcium phosphate cements. Biomaterials 2002;23:4167–4176.

23. Ge Z, Baguenard S, Lim LY, Wee A, Khor E. Hydroxyapatite-chitin materials as potential tissue engineered bone substitutes. Biomaterials 2004;25:1049–1058.

24. Hockin HKX, Carl GSJ. Fast setting calcium phosphate-chitosan scaffold: mechanical properties and biocompatibility. Biomaterials 2005;26:1337–1348.

25. Zhang L, Li YB, Zhou G, Lu GY, Zuo Y. Investigation on the setting mechanism of nano-hydroxyapatite/chitosan bone cement (in Chinese). J Inorgan Mater 2006;21:1197–1202.

26. Gbureck U, Barralet JE, Spatz K, Grover LM, Thull R. Ionic modification of calcium phosphate cment viscosity. Part I: hypodermic injection and strength improvement of apatite cement. Biomaterials 2004;25:2187–2195.

27. Oyane A, Kim HM, Furuya T, Kokubo T, Miyazaki T, Nakamura T. Preparation and assessment of revised simulated body fluids. J Biomed Mater Res A 2003;65A:188–195.

28. Yoshikawa M, Hayami S, Toda T. In vivo estimation of calcium phosphate cements containing chondroitin sulfate in subcutis. Mater Sci Eng C 2002;20:135–141.

29. Frayssinet P, Gineste L, Conte P, Fages J, Rouquet N. Short-term implantation effects of a DCPD-based calcium phosphate cement. Biomaterials 1998;19:971–977.

30. Lewis G. Properties of acrylic bone cement: state of the art review. J Biomed Mater Res 1997;38:155–182.

31. Wei H, Kenneth EG, Nikola B, Dave BP, Emily A, Michael H. Micro/nanomachining of polymer surface for promoting osteoblast cell adhesion. Biomed Microdevices 2003;5: 101–108.

32. Chou YF, Chiou WA, Xu Y, Dunn JCY, Wu BM. The effect of pH on the structural evolution of accelerated biomimetic apatite. Biomaterials 2004;25:5323–5331.

33. Uchida M, Kim HM, Miyaji F, Kokubo T, Nakamura T. Apatite formation on zirconium metal treated with aqueous NaOH. Biomaterials 2002;23:313–317.

34. Khairoun I, Driessens FC, Boltong MG, Planell JA, Wenz T. Additional of cohesion promotors to calcium phosphate cements. Biomaterials 1999;20:393–398.

35. Khairoun I, Boltong MG, Driessens FCM, Planell JA. Some factors controlling the injectability of calcium phosphate bone cements. J Mater Sci Mater Med 1998;9:425–428.

36. Miyamoto Y, Ishikawa K, Takechi M, Toh T, Yuasa T, Nagayama M, et al. Histological and compositional evaluations of three types of calcium phosphate cements when implanted in subcutaneous tissue immediately after mixing. J Biomed Mater Res (Appl Biomater) 1999;48:36–42.

37. Leroux L, Hatim Z, Lacout JL. Effects of various adjuvants (lactic acid, glycerol, and chitosan) on the injectability of a calcium phosphate cement. Bone 1999;25:31S–34S.

38. Ueyama Y, Ishikawa K, Mano T, Koyama T, Nagatsuka H, Matsumura T, et al. Initial tissue response to anti-washout apatite cement in the rat palatal region: comparison with conventional apatite cement. J Biomed Mater Res 2001;55: 652–660.

39. Bohner M, Baroud G. Injectability of calcium phosphate pastes. Biomaterials 2005;26:1553–1563.

40. Hernández L, Fernández M, Collía F, Gurruchaga M, Goñi I. Preparation of acrylic bone cements for vertebroplasty with bismuth salicylate as radiopaque agent. Biomaterials 2006;27: 100–107.

41. Sarda S, Fernández E, Llorens J, Martínez S, Nilsson M. Rheological properties of an apatite bone cement during initial setting. J Mater Sci Mater Med 2001;12:905–909.

42. Tangpasuthadol V, Pongchaisirikul N, Hoven VP. Surface modification of chitosan films: effects of hydrophobicity on protein adsorption. Carbohydr Res 2003;338:937–942.

43. Zanchetta P, Guezennec J. Surface thermodynamics of osteoblasts: relation between hydrophobicity and bone active biomaterials. Colloid Surf B: Biointerf 2001;22:301–307.

44. Zhang M, Li XH, Gong YD, Zhao NM, Zhang XF. Properties and biocompatibility of chitosan films modified by blending with PEG. Biomaterials 2002;23:2641–2648.

45. Neo M, Nakamura T, Ohtsuki C, Kokubo T, Yamamuro T. Apatite formation on three kinds of bioactive materials at an early stage in vivo: a comparative study by transmission electron microscopy. J Biomed Mater Res 1993;27:999–1006.

46. Li Z, Yubao L, Aiping Y, Xuelin P, Xuejiang W, Xiang Z. Preparation and in vitro investigation of chitosan/nano-hydroxyapatite composite used as bone substitute materials. J Mater Sci Mater Med 2005;16:213–219.

47. Kokubo T. Formation of biologically active bone-like apatite on metals and polymers by a biomimetic process. Thermochim Acta 1996;280/281:479–490.

48. Kokubo T. Surface chemistry of bioactive glass-ceramics. J Non-Cryst Solids 1990;120:138–151.

49. Zhao W, Wang J, Zhai W, Wang Z, Chang J. The self-setting properties and in vitro bioactivity of tricalcium silicate. Biomaterials 2005;26:6113–6121.

50. Méndez JA, Fernández M, González-Corchón A, Salvado M, Collía F, de Pedro JA, Levenfeld BL, López-Bravo A, Vázquez B, San Román J. Injectable self-curing bioactive acrylic-glass composites charged with specific anti-inflammatory/analgesic agent. Biomaterials 2004;25:2381–2392.

51. Wolke JGC, Ooms EM, Jansen JA. In vivo resorption behavior of a high strength injectable calcium-phosphate cement. Bioceram Key Eng Mater 2000;192:793–796.

52. Yang Q, Troczynski T, Liu D. Influence of apatite seeds on the synthesis of calcium phosphate cement. Biomaterials 2002;23:2751–2760.

53. Chow LC, Takagi S, Ishikawa K. Formation of hydroxyapatite in cement systems. In: Brown PW, editor. Hydroxyapatite and Related Materials. Boca Raton: CRC Press, 1994. p 127–137.

54. Takagi S, Chow LC, Ishikawa K. Formation of hydroxyapatite in new calcium phosphate cements. Biomaterials 1998;19:1593–1599.

55. Zhang Y, Zhang MQ. Synthesis and characterization of macroporous chitosan/calcium phosphate composite scaffolds for tissue engineering. J Biomed Mater Res 2001;55:304–312.

56. Sundararajan VM, Howard WTM. Porous chitosan scaffolds for tissue engineering. Biomaterials 1999;20:1133–1142.

57. Wan ACA, Khor E, Hastings GW. Preparation of a chitin-apatite composite by in situ precipitation onto porous chitin scaffolds. J Biomed Mater Res 1998;41:541–548.

58. Ohtsusi C, Kokubo T, Yamamuro T. Mechanism of apatite formation on CaO-SiO$_2$-P$_2$O$_5$ glasses in simulated body fluid. J Non-Cryst Solids 1992;143:84–92.

59. Wang XX, Hayakawa S, Tsuru K, Osaka A. A comparative study of in vitro apatite deposition on heat-, H$_2$O$_2$-, and NaOH-treated titanium surfaces. J Biomed Mater Res 2001;54:172–178.

60. Miyazaki T, Kim HM, Miyaji F, Kokubo T, Kato H, Nakamura T. Bioactive tantalum metal prepared by NaOH treatment. J Biomed Mater Res 2000;50:35–42.

61. Kato H, Nakamura T, Nishiguchi S, Fujita H, Miyazaki T, Miyaji F, Kim HM, Kokubo T. Bonding of alkali- and heat-treated tantalum implants to bone. J Biomed Mater Res B Appl Biomater 2000;53:28–35.

62. Uchida M, Kim HM, Miyaji F, Kokubo T, Nakamura T. Apatite formation on zirconium metal treated with aqueous NaOH. Biomaterials 2002;23:313–317.

63. Bettger WJ, O'Dell BL. Physiological roles of zinc in the plasma membrane of mammalian cells. J Nutr Biochem 1993;4:194–207.

64. Yamaguchi M, Ehara Y. Zinc decrease and bone metabolism in the femoral-metaphyseal tissues of rats with skeletal unloading. Calcif Tissue Int 1995;57:218–223.

65. Yamaguchi M, Oishi H, Suketa Y. Zinc stimulation of bone protein synthesis in tissue culture. Biochem Pharmacol 1988;37:4075–4080.

66. Kanzaki N, Onuma K, Treboux G, Tsutsumi S, Ito A. Inhibitory effect of magnesium and zinc on crystallization kinetics of hydroxyapatite (0001) face. J Phys Chem B 2000;104:4189–4194.

67. Kanzaki N, Onuma K, Treboux G, Tsutsumi S, Ito A. Effect of impurity on two-dimensional nucleation kinetics: case studies of magnesium and zinc on hydroxyapatite (0001) face. J Phys Chem B 2000;105:1991–1994.

68. Ito A, Kawamura H, Otsuka M, Ikeuchi M, Ohgushi H, Ishikawa K, Onuma K, Kanzaki N, Sogo Y, Ichinose N. Zinc-releasing calcium phosphate for stimulating bone formation. Mater Sci Eng C 2002;22:21–25.

69. Ishikawa K, Miyamoto Y, Yuasa T, Ito A, Magayama M, Suzuki K. Fabrication of Zn containing apatite cement and its initial evaluation using human osteoblastic cells. Biomaterials 2002;23:423–428.

70. Ooms EM, Wolke JGC, van de Heuvel MT, Jeschke B, Jansen JA. Histological evaluation of the bone response to calcium phosphate cement implanted in cortical bone. Biomaterials 2003;24:989–1000.

71. Wang XH, Ma JB, Wang YN, He BL. Bone repair in radii and tibias of rabbits with phosphorylated chitosan reinforced calcium phosphate cements. Biomaterials 2002;23:4167–4176.

72. Miyamoto Y, Ishikawa K, Takechi M, Toh T, Yuasa T, Nagayama M, Suzuki K. Histological and compositional evaluations of three types of calcium phosphate cements when implanted in subcutaneous tissue immediately after mixing. J Biomed Mater Res B Appl Biomater 1999;48:36–42.